Surface Science Letters

A LEED structural analysis of the Co(10$\bar{1}$0) surface

H. Over, G. Kleinle, G. Ertl

Fritz-Haber-Institut der Max-Planck-Gesellschaft, W-1000 Berlin 33, Germany

W. Moritz

Institut für Kristallographie und Mineralogie, Universität München, W-8000 München 2, Germany

K.-H. Ernst, H. Wohlgemuth, K. Christmann and E. Schwarz

Institut für Physikalische und Theoretische Chemie, FU Berlin, W-1000 Berlin 33, Germany

The structure of the clean Co(1010) surface has been analysed by LEED. Application of a recently developed computational scheme reveals the prevalence of the termination A in which the two topmost layers exhibit a narrow spacing of 0.62 Å, corresponding to a 12.8($\pm$0.5)% contraction with respect to the bulk value, while the spacing between the second and third layer is slightly expanded by 0.8($\pm$0.2)%.

The (10$\bar{1}$0) surface of a hcp crystal represents the counterpart to the well-known (110) plane of fcc crystals. In contrast to the latter, however, so far only one structural analysis (for Re (10$\bar{1}$0)) has been reported in the literature [1]. As a peculiarity, this kind of surface may exhibit two types of termination as illustrated in fig. 1. The coordination of the topmost atoms differs for the two terminations. In termination A each atom of the top layer is surrounded by four nearest neighbours in the second layer with a relatively small layer spacing. Modifaction B shows a surface atom surrounded by only two nearest neighbours in the second layer with much larger spacing between the two topmost layers. Termination B obviously exhibits a much stronger surface corrugation, and pronounced relaxation effects in the topmost layers are most likely. The differing corrugations of the two surface terminations provide quite different adsorption sites.

In contrast to other transition metals relatively few investigations have dealt with cobalt single crystal surfaces. Concerning the hexagonal Co phase LEED investigations were reported only for the (0001) [2–4] and for the (11$\bar{2}$0) surface [5]. In this work we present a LEED structure analysis of the clean Co(10$\bar{1}$0) surface. The analysis was carried out applying the automatic optimization scheme and the r_{DE}-factor developed by Kleinle et al. [6], final results were cross-checked with standard r-factor methods.

The experiments were carried out in a standard UHV chamber at a base pressure $p < 10^{-8}$ Pa. Details about the experimental setup are described elsewhere [7]. The cobalt single crystal with a size of 6 mm diameter and 1 mm thickness was orientated within 0.5° in the [10$\bar{1}$0] direction by Lamprecht GmbH, D-7531 Neuhausen. After mechanical polishing the crystal was electrochemically etched as described by Welz et al. [5] resulting in a mirror-like finish. Thereafter the crystal was demagnetized by a Helmholtz coil, spot-welded between two tantalum wires and attached to a sample manipulator. The crystal was adjusted on the sample manipulator in a way to allow normal incidence within 0.5°. The crystal temper-
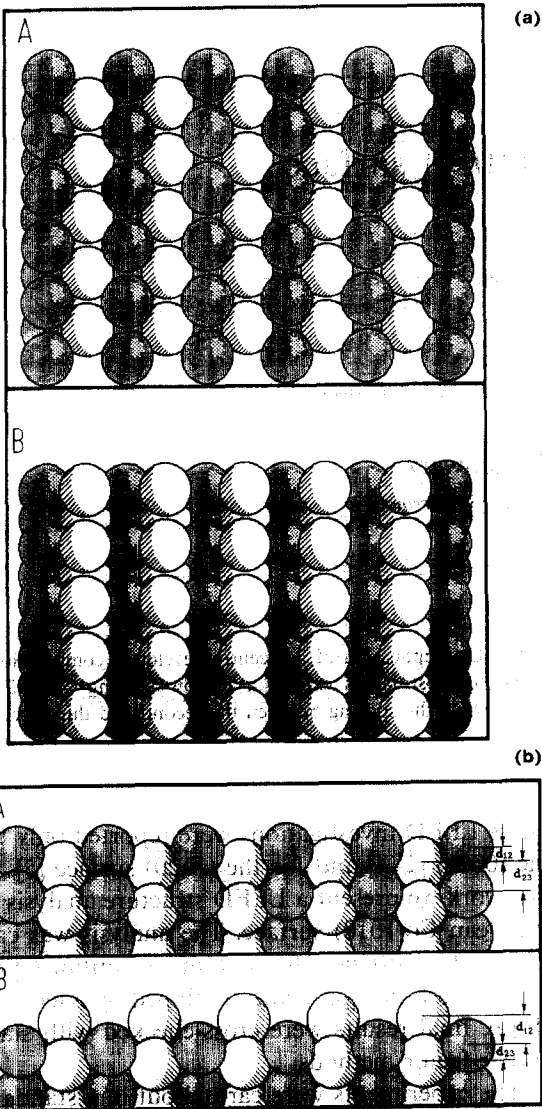
(a)

(b)

Fig. 1. (a) Top- (b) side-view of the two possible terminations (A,B) of a hcp (10$\overline{1}$0) surface.

Fig. 2. LEED-pattern of the clean Co(10$\overline{1}$0) surface at an electron energy $E_0 = 66$ eV.

care was taken not to reach sample temperatures above 680 K. After numerous sputter–annealing cycles only small amounts of carbon remained at the surface which could be reactively removed by oxygen at 650 K. Traces of oxygen impurity could be reacted off by hydrogen at 680 K. The cleanliness of the surface could be controlled very sensitively by HREELS. A LEED pattern of the clean surface at an electron energy $E_0 = 66$ eV is shown in fig. 2.

LEED I/V curves were measured and recorded by means of a video ("auto") LEED system devel-

ature could be controlled by a NiCi–Ni thermocouple spot-welded to the edge of the sample.

Further crystal preparation in vacuum consisted of cycles of argon sputtering at 300–500 eV ion energy and beam currents of 3–6 μA/cm^2 whereby the sample temperature was successively increased up to 500 K followed by cycles of annealing at 680 K. Since a phase transition from the hcp to the fcc phase occurs at 700 K much
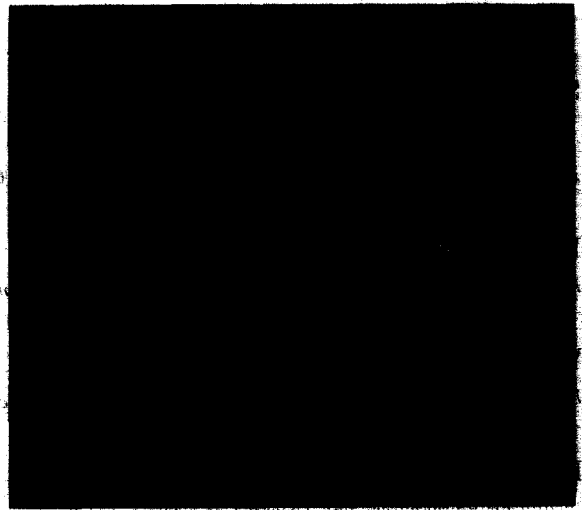

Fig. 3. Experimental I/V curves of four symmetry-equivalent LEED-beams: (1.2), (1.$\overline{2}$), ($\overline{1}$.2) and ($\overline{1}$.$\overline{2}$).

oped at the University of Erlangen [8]. Normal incidence of the primary beam was carefully adjusted as demonstrated by fig. 3, which displays I/V curves of four symmetry-equivalent LEED spots ((1,2), (1,$\bar{2}$), ($\bar{1}$,2), ($\bar{1}$,$\bar{2}$)). Small deviations from normal incidence lead to non-equivalence of the I/V curves. For each beam an average of all experimentally accessible equivalent beams was taken.

The LEED calculations were performed utilizing the layer doubling scheme [9] to describe the interlayer multiple scattering. The two layers having an interlayer spacing of only 0.718 Å were treated as a composite layer for which the multiple-scattering equations were solved in angular momentum space. The number of angular momentum components was reduced by the use of symmetry-adapted functions [10]. Electron scattering at the ion cores was described in the muffin-tin approximation, using up to nine phase shifts for Co. The corresponding atomic potential was obtained from band structure calculations and has been successfully used in the LEED analysis of Co(0001) [3,4], Co(111) [4], Co(100) [11] and Co-(11$\bar{2}$0) [5]. Further nonstructural parameters in this analysis included an energy-dependent imaginary part of the inner potential $V_i = 0.85(E + V_{or})^{1/3}$. The thermal vibrations were taken into account by a Debye temperature of 450 K for all layers. The energy dependence of the real part of the inner potential was considered by a square root behaviour according to a theoretical calculation for the free electron gas [12]. Up to 33 symmetrically non-equivalent beams were used in the layer doubling scheme. For comparison with model calculations eight LEED spots of the clean Co (10$\bar{1}$0) surface ((1,0), (0,1), (1,1), (0,2), (2,1), (0,3), (1,2), (2,0)) were investigated in the energy range between 70 and 380 eV.

The agreement between experimental J^{ex} and theoretical intensity J^{th} data was measured by the r_{DE}-factor introduced by Kleinle et al. [11]. This r-factor requires only a small set of data points at discrete energies. The step width on the energy scale can be taken up to 20 eV, which provides a considerable reduction in the computing time. The main advantage, however, is that it allows to apply nonlinear least squares optimization procedures

for simultaneous refinement of structural parameters. The r_{DE}-factor is given by:

$$r_{DE} = \sum_g w_g \frac{\sum_i \left| J_i^{ex} - c_g J_i^{th} \right|^2}{\sum_i J_i^{ex}}.$$

For each beam $g(=h,k)$ the summation i is performed over the n_g data points at energies i, whereby the scaling factor

$$c_g = \sum_{i=1}^{g} J_i^{ex} \bigg/ \sum_{i=1}^{n_g} J_i^{th},$$

normalizes the absolute intensities J_i for each of the individual beams. The contribution from each beam is weighted with the factor

$$w_g = n_g \bigg/ \sum_g n_g.$$

The optimization method which was applied here is a nonlinear least squares fit procedure which combines the expansion method with the method of the steepest descent [13]. A full description of the method is given in ref. [14].

This method requires the partial derivatives of the intensities with respect to the structural parameter. In the program version of Kleinle [15] the derivatives were evaluated numerically by full-dynamical calculations. Influenced by the Tensor LEED-approximation [16], an approximate calculation of derivatives for structural parameters of the composite layer was implemented in the program [17,18].

The stacking of the layer matrices is achieved by a linear approximation whereby the once inverted matrices are exploited in the evaluation of all derivatives. Hence, the actual computing time for determining a surface structure is nearly independent of the number of optimizing structural parameters. A detailed description will be given elsewhere [18]. The direct application of Tensor LEED is not possible, because the composite-space method does not give any access to the LEED wavefunction in the vicinity of each displaced atom.

In the present analysis up to 7 layer spacings were taken as variable parameters and addition-

ally the constant part of the muffin-tin zero. Note that the computational effort is nearly independent of the number of structural parameters. However, only the top two layer spacings exhibited a detectable deviation from the bulk value. The calculations were restricted to the energy range of 70–380 eV (step width 15 eV) and did not fully use the experimental data base (up to 600 eV) in order to save computer time.

The step width of 15 eV corresponds to 21 points on the energy scale and a total number of 146 data points in 8 beams. This data base is highly sufficient to determine 8 free parameters according to previous investigations at related systems [6,19]. An attempt to determine the minimum data base by variation of the step width was not undertaken.

In order to tackle the question which of the two terminations represents the stable configuration of this surface the automatic fit procedure described above was carried out for both models. Each model started from the truncated bulk structure. The process converged rapidly. Final results were attained after 4 iteration cycles when all parameters were within limits of 0.01 Å. Furthermore extensive tests were performed which demonstrated that the lattice parameters obtained by our optimizing scheme do not depend on the starting configuration within the error bars of 0.01 Å. The corresponding r_{DE}-factors resulted in 0.24 for termination A, and 0.48 for termination B.

For the final results full curves in 3 eV steps and two standard r-factors (Zanazzi–Jona [20] and Pendry [21]) were calculated. All three r-factors exhibit a clear preference for termination A as shown in table 1. The results are presented in fig. 4 together with the experimental I–V curves and demonstrate the reliability of this structural determination. The sensitivity of the first two layer spacings upon our structural input parameters is
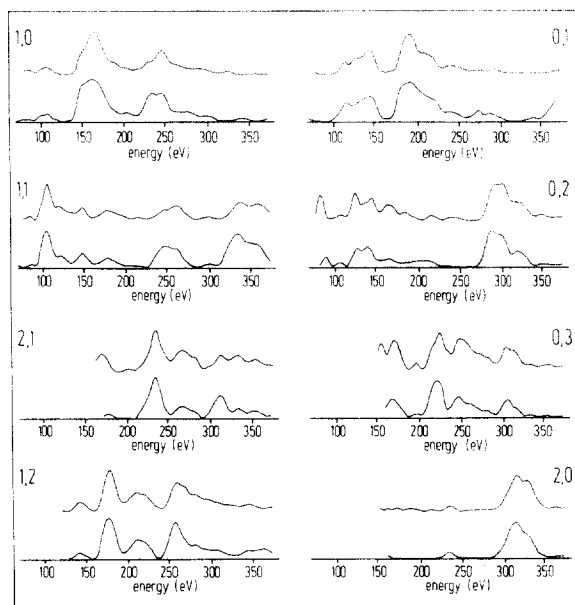

Fig. 4. Calculated (upper) and experimental (lower) I/V curves of 8 non symmetry-equivalent LEED-beams in the energy range between 70 and 380 eV.

demonstrated by the r_{DE}-factor contour-plot in fig. 5 [22].

It is interesting to note that in spite of the poor agreement for termination B, the layer spacings for both terminations agree quite well, but with additional rows of Co-atoms for termination B (see fig. 1b). A coexistence of both surface structures either in small or in large domains seems to be possible requiring a mixture of diffraction intensities or amplitudes, respectively. However, no improvement could be achieved by mixing the intensities of termination B with the intensities of termination A. The lower limit of the concentration of termination B which produced a detectable worsening of the r-factor was about 10%. In summary, it appears as if termination B does not exist on the Co(10$\bar{1}$0) surface to within the limits of the present analysis. It should be noted that the rather good r-factor of Zannazzi–Jona, especially for termination B, originates from the inherent artefact, whereafter a large energy range under investigation causes a small corresponding value of r_{ZJ} [15] and vice versa.

It is well known [23] that less close-packed clean metal surfaces exhibit measurable relaxa-
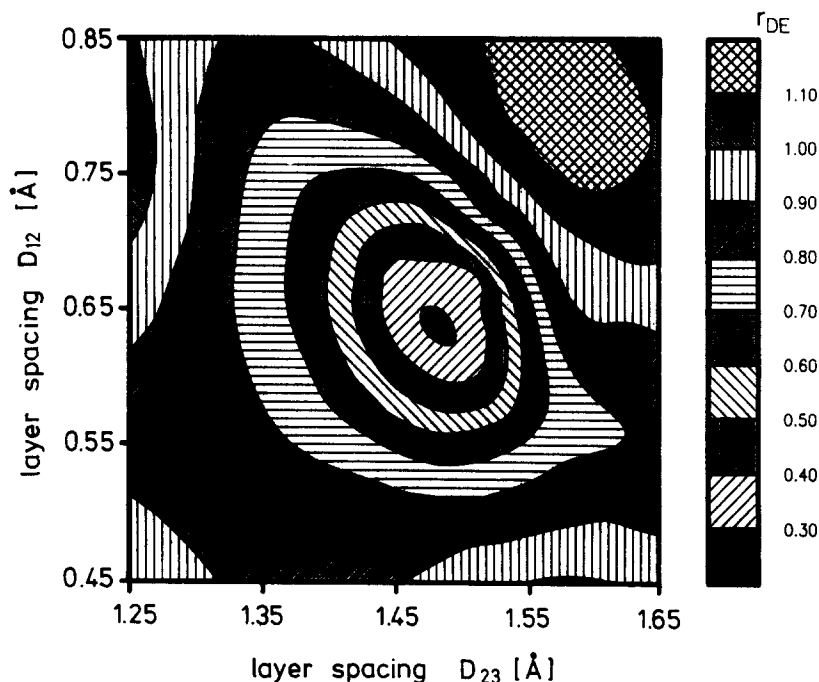
Table 1
Comparison of r-factors (r_{DE}, r_{ZJ}, r_P) for both configurations of the Co (10$\bar{1}$0) surface

Termination	r_{DE}	r_{ZJ}	r_P
A	0.240	0.090	0.310
B	0.480	0.137	0.720

Fig. 5. Plot the r_{DE}-factor as a function of the first two layer spacings d_{12} and d_{23} as defined in fig. 1b [22].

tions, namely, a contraction between the first and second atomic layers followed by an expansion between the next two layers. Such relaxations can continue well into the bulk, but their magnitude decays exponentially with depth. Therefore up to seven layer spacings were simultaneously optimized. The main result is a contraction of the first layer spacing d_{12} down to 0.625 ± 0.003 Å. That is 12.8(±0.5)% less than the truncated bulk value which, however, represents only a 1.3% decrease in the bond length between neighbours in the first compound layer from 2.889 to 2.857 Å. The second layer spacing d_{23} is only slightly expanded to 1.458 ± 0.003 Å, and the third layer spacing d_{34} corresponds to the bulk value within the limits of

uncertainty. Table 2 shows the calculated layer spacings between the first seven layers below the surface. Hence the strong contraction within the first (compound) layer decayed after one or two layers.

In table 3 we compare our results with multi-layer relaxation parameters for other open surfaces such as Cu(110) [24], Al(110) [25], Re(10$\bar{1}$0) [1] and Fe(211) [26]. Clearly, the contraction found here is in good agreement with these observations. Only Re(10$\bar{1}$0) displays a significantly higher contraction of 17%, however, only three beams were analysed in the corresponding analysis [1], leading to an uncertainty of about 5%. It is most remark-able that the variation of bond length coincides

Table 2
Calculated layer spacings between the first seven layers below the surface

Layer spacing	d_{12}	d_{23}	d_{34}	d_{45}	d_{56}	d_{67}	d_{78}
(Å)	0.625 ± 0.003	1.458 ± 0.003	0.722 ± 0.005	1.436 ± 0.010	0.724 ± 0.016	1.403 ± 0.055	0.730 ± 0.04

Table 3
Comparison of multilayer relaxations Δd_{12} and Δd_{23} for some rectangular single crystal surfaces

	Cu(110) [24]	Al(110) [25]	Re(10T0) [1]	Fe(211) [26]	Co(1010)
$\Delta d_{12}/d_{12}$	$-8.5(\pm 0.7)\%$	$-8.4(\pm 0.8)\%$	-17%	-10%	$-12.8(\pm 0.5)\%$
$\Delta d_{23}/d_{23}$	$+2.3(\pm 0.9)\%$	$+4.9(\pm 1.0)\%$	$+1-2\%$	$+5\%$	$+0.76(\pm 0.2)\%$

for both crystals Re(10T0) and Co(10T0) indicating a similar relaxation mechanism for these hcp surfaces.

To summarize, our LEED analysis of the clean Co(10T0) surface reveals that only termination A represents the stable atomic configuration in the surface, exhibiting a contraction of the first subplane spacing by 12.8($\pm$0.5)% and no further relaxation deeper in the bulk. We note that the same termination (A) was found previously for the clean Re(10T0) surface [1].

We thank Dr. A. Preusser for technical assistance.

Note added in proof

After acceptance of our Letter a recent LEED analysis from Lindroos et al. [27] concerning "The termination and multilayer relaxation at the Co-(10T0) surface" was brought to our knowledge. The I/V curves of Lindroos et al. are in good agreement with our results, but a discrepancy occurs with respect to the magnitude of the first layer contraction. While Lindroos et al. ascertained a contraction of $-6.5(\pm 2)\%$ we determined a larger contraction of $-12.8(\pm 0.5)\%$.

References

[1] H.L. Davis and D.M. Zehner, J. Vac. Sci. Technol. 17 (1980) 190.
[2] G.L.P. Berning, Surf. Sci. 61 (1976) 673.
[3] G.L.P. Berning, G.P. Alldredge and P.E. Viljoen, Surf. Sci. 104 (1981) L225.
[4] B.W. Lee, R. Alsenz, A. Ignatiev and M.A. Van Hove, Phys. Rev. B 17 (1978) 1510.
[5] M. Welz, W. Moritz and D. Wolf, Surf. Sci. 125 (1983) 473.
[6] G. Kleinle, W. Moritz, D.L. Adams and G. Ertl, Surf. Sci. 219 (1989) L637.
[7] K.-H. Ernst, E. Schwarz and K. Christmann, in preparation.
[8] K. Müller and K. Heinz, in: The Structure of Surfaces, Eds. S.Y. Tong and M.A. Van Hove (Springer, Berlin, 1986) p.105.
[9] M.A. Van Hove and S.Y. Tong, Surface Crystallography by LEED, Springer Series in Chemical Physics (Springer, Berlin, 1979).
[10] W. Moritz, J. Phys. C 17 (1984) 353.
[11] M. Maglietta, E. Zanazzi, F. Jona, D.W. Wepsen and P.M. Marcus, Appl. Phys. 15 (1978) 409.
[12] L. Hedin and B.I. Lundquist, J. Phys. G 4 (1971) 2064.
[13] D.W. Marquardt, J. Sol. Indust. Appl. Math. 11 (1963) 431.
[14] G. Kleinle, W. Moritz and G. Ertl, Surf. Sci. 238 (1990) 119.
[15] G. Kleinle, Thesis, Freie Universität Berlin (1989).
[16] (a) P.J. Rous, J.B. Pendry, D.K. Saldin, K. Heinz, K. Müller and N. Bickel, Phys Rev. Lett. 57 (1986) 2950;
(b) P.J. Rous and J.B. Pendry, Comput. Phys. Commun. 54 (1989) 137.
[17] W. Moritz, H. Over, G. Kleinle, G. Ertl, in: The Structure of Surfaces III, Eds. M.A. Van Hove, S.Y. Tong and Xie Xide (Springer, Berlin, 1990) in press.
[18] H. Over, U. Ketterl, W. Moritz and G. Ertl, in preparation.
[19] G. Kleinle, J. Wintterlin, G. Ertl, R.J. Behm, F. Jona and W. Moritz, Surf. Sci. 225 (1990) 171.
[20] E. Zanazzi and F. Jona, Surf. Sci. 62 (1977) 61.
[21] J.B. Pendry, J. Phys. C 13 (1980) 937.
[22] A. Preusser, Comput. Aided Geom. Design 3 (1986) 267.
[23] D.L. Adams, W.T. Moore and K.A.R. Mitchell, Surf. Sci. 149 (1985) 407.
[24] D.L. Adams, H.B. Nielsen, J.N. Andersen, I. Steensgaard, R. Feidenhans'l and J.E. Sørensen, Phys. Rev. Lett. 49 (1982) 669.
[25] H.B. Nielsen, J.N. Andersen, L. Petersen and D.L. Adams, J. Phys. C. 15 (1982) L1113.
[26] J. Sokolov, H.D. Shih, U. Bardi, S. Jona and P.M. Marcus, Solid State Commun. 48 (1983) 739.
[27] M. Lindroos, C.J. Barnes, P. Hu and D.A. King, Chem. Phys. Lett. 173 (1990) 92.